RESEARCH ARTICLE

Synthesis, Characterization, and Adsorption Properties of Highly Microporous Structured Activated Carbon

İlhan KÜÇÜK[1,2] ✉ iD **, Yunus ÖNAL[3]** ✉ iD

[1] Department of Chemistry, Faculty of Art and Science, Inonu University, 44280 Malatya, Turkey
[2] Muş Alparslan University, 49250, Muş, Turkey
[3] Department of Chemical Engineering, Faculty of Engineering, Inonu University, 44280 Malatya, Turkey

Abstract: The aim of this study is to synthesize activated carbon with high surface area from peach kernel shells which is an agricultural waste. In this study, activated carbon synthesis was carried out by using CO_2 at 2 different temperatures (800 and 900 °C) with physical activation from products carbonized at 4 different temperatures (300, 400, 500, and 600 °C) and 2 different N_2 gas flow rates (100 and 500 mL/min). After carbonization, solid, liquid, and gas yields of the materials were calculated. The surface area of activated carbons synthesized was calculated by BET analysis and the differences in the surface area were shown by changing the synthesis conditions. Surface areas vary between 340.15 and 686.74 m^2/g. In samples pores formed were examined by DFT plus. It was found that most of these pores consist of micropores. Also, the structures of the samples were examined with SEM and XRD analyses. Methylene blue removal of the synthesized samples was studied and the results were compared.

INTRODUCTION

Activated carbon, known as activated charcoal, is a high surface area, amorphous and graphite-free carbonaceous compound. Activated carbons, which do not have a chemical formula, differ from each other with their surface areas, advanced and adjustable pores, mechanical strength, high reactive surface chemistry, adsorption capacities, the raw materials they are synthesized, the activation method used and chemicals used (1-5).

One of the most important properties of activated carbons is that they have a porous structure that causes the surface area to grow. Besides its porous structure, pore volume and diameter are important. The formation of pores in activated carbons starts at the carbonization stage. Through physical and chemical activation, these pores gain volume and open if there are closed pores. The formation of the pores is as follows (6):

✓ Volatile components in the raw material leave the structure by heating the raw material in an inert environment.

✓ These components, which move away from the raw material, pore on the raw material according to the size of the structure.

✓ If the displaced structure is in the middle of the solid, the internal pressure will increase in the solid and will open micro channels as this structure moves away.

The pore distribution and pore diameter in an activated carbon vary depending on the type of raw material used and the carbonization temperature (7).

In recent years, research has been increased towards the use of agricultural waste products for the synthesis of activated carbon. These biomass products are sustainable, cheap, and rich sources of carbon. This feature makes them the suitable raw material for the synthesis of activated carbon. In respect of environmental concern, these agricultural wastes will get decayed finally with time, but most of them reduce slowly and create pollution. The best way to address these issues is to use them as precious material. Along with having a good source of carbon, these biomaterial wastes include other elements and compounds, which can be exploited cleverly according to the application (8). Some agricultural wastes synthesized from activated carbon coffee husks (9), durian shells (10), olive stones (11), rice straw (12), oil palm fibers (13), walnut shells (14), rice husks (15), waste apricot (16), cherry stones (17), banana peels (18), sawdust (19), rice bran (20), almond shells (21), tea waste (22), herb residues (23), corn cobs (24), rice hulls (25), sugarcane bagasse (26), cotton stalks (27), orange peels (28), date stones (29), coconut husks (30), etc.

Activated carbon is an adsorbent acquired from carbonaceous substances with a disorganized crystallographic shape, constituted through randomly dispensed microcrystals. This microcrystalline shape is constructed from standard systems which include graphene sheets and fullerene or quasi-graphitic fragments. However, this microcrystalline association does now no longer enlarge on a macroscopic scale ensuing in a disordered and surprisingly nanoporous shape. Consequently, those substances gift excessive surface area, extensive type of practical groups and a pore length distribution. All those traits supply them an outstanding potential to adsorb a remarkable range of molecules (31). In addition to this potential, it is used in many different fields. Some of those purification (32), nuclear power stations (33), gas separation (34), energy storage (35), catalysis (36), water treatment (37), pharmaceutical (38), capacitors (39), petroleum industries (40), etc.

Adsorption, which is one of the most used areas of activated carbons, takes place through the pores on the surface of the activated carbon. The substance to be adsorbed enters through these pores and interacts with the outer surface of the activated carbon and adheres to that region. Adsorption takes place in this manner. However, for the adsorption to take place, the material to be adsorbed must pass through the pores of the activated carbon. If these pores are small or if the material to be adsorbed is larger than the pores, adsorption cannot take place (41).

In this study, activated carbon synthesis was made from peach kernel shells which are agricultural waste. In this study, carbonization temperature, carbonization gas flow and activation temperature were changed. The synthesized active carbons were compared with each other.

EXPERIMENTAL

Synthesis of the Activated Carbon
Supplied with peach kernel shells (Bursa, Turkey) was used without applying any pretreatment except for washing with water. These shells were firstly subjected to pyrolysis process and the synthesis of activated carbon was made on solid char. A three-zone furnace was used for the pyrolysis process of peach kernel shell. The furnace was placed in the steel reactor with the help of a steel cuvette by taking approximately 500 ± 25 g and subjected to pyrolysis in nitrogen atmosphere. Pyrolysis was carried out at 300, 400, 500, and 600 °C. The furnace started at room temperature and increased to 10 °C per minute to the final temperature. When it reached the final temperature, the furnace remained stable for 1 hour and was then allowed to cool to room temperature. Nitrogen gas atmosphere was used in all of these processes and nitrogen gas flow was made with the help of a manometer. Nitrogen gas for the samples was tested by means of manometer pyrolysis at 100 and 500 mL/min gas flow rates. The pyrolysis liquid was collected by means of the back cooler connected to the outlet end of the steel reactor.

Char obtained was placed in a three-zone furnace by means of a glass reactor and the physical activation was carried out. Two different activation temperatures (800 and 900 °C) were studied. At these temperatures, CO_2 gas was used for activation and the gas flow was fixed to a flow of 100 mL/min by means of a manometer. In this activation process, the furnace increased from 10 °C per minute starting from room temperature and remained at the final temperature for 1 hour.

Preparation of Methylene Blue
The methylene blue used in the study was placed in a beaker and kept in an oven at 105° for 6 hours. Then 1 gram of methylene blue was taken and 1000 ppm, 1 liter stock solution was prepared.

Adsorption
The prepared stock solution was diluted to 100 ppm and 0,1 grams of activated carbon sample was added to 100 mL and mixed for approximately 24 hours by magnetic stirrer (pH 6.2 at room temperature). The received solutions were filtered through a syringe filter and measured at 660 nm in a UV-Vis device.

Equipment
Carbonization process with Protherm PZF 12/50/700 furnace, activation process with Protherm PZF 12/60/600 furnace were carried out.

Analysis

UV-Vis analyses were performed with a Shimadzu UV-2100S, SEM analyses were carried out with a Leo EV040 brand scanning electron microscope, XRD were realized with a Rigaku RadB-DMAX II computer-controlled X-ray diffractometer, and BET (Brunauer-Emmett-Teller) measurements were performed with a Micromeritics Tristar 3000, and elemental analyses were realized with a CHNS-932 (LECO) Elemental Analyzer.

RESULTS AND DISCUSSION

Biomass is converted to solid (char), liquid, and gas by pyrolysis process. These transformations vary depending on the biomass species and pyrolysis conditions. Table 1 shows the solid, liquid, and gas transformations of the peach kernel shell used as raw material as a result of the process.

Table 1: Solid, liquid and gas yields as a result of pyrolysis process.

Temperature / N_2 Gas Flow	Solid Yield %	Liquid Yield %	Gas Yield %
300 °C/ 100 mL/min	41.5	39.91	18.59
300 °C/ 500 mL/min	43.02	37.55	19.43
400 °C/ 100 mL/min	34.24	37.04	28.72
400 °C/ 500 mL/min	33.62	34.22	32.16
500 °C/ 100 mL/min	29.55	33.1	37.35
500 °C/ 500 mL/min	29.01	36.17	34.82
600 °C/ 100 mL/min	27.03	37.25	35.72
600 °C/ 500 mL/min	27.03	31.29	41.68

Peach kernel shell was subjected to pyrolysis at four different temperatures (300, 400, 500, and 600 °C) and solid, liquid and gas yields were calculated. Solid yield decreased with increasing temperature. It is seen that gas yield increases while liquid yield decreases with increasing temperature. Although the change in pyrolysis gas flow rate changed the solid, liquid and gas yields excessively at some temperatures, the change in some temperatures was very low.

The BET analysis results of the synthesized activated carbons are shown in Table 2. According to these results, the surface area varies between 686.74 and 340.15 m^2/g. The highest surface area was achieved at an activation temperature of 800 °C in N_2 gas flow of 100 mL/min at 500 °C carbonization temperature. Table 2 shows that the change in temperature of pyrolysis caused changes in surface areas. Increasing the pyrolysis temperature up to 500 °C caused a positive change in the surface areas, while the rise to 600 °C showed a negative change in the surface areas. The change in the gas flow rate of pyrolysis caused changes in the samples. There was no order in these changes. The increased gas flow rate, except for 2 samples, caused a decrease in surface areas. The change in the activation temperature caused the surface area to change. In particular, the increase in activation temperature increased the surface area of samples. Since one of the objectives in activated carbons is the increased surface, it is necessary to work at high activation temperature when using CO_2 for high surface area activated carbons. Also, when we look at the synthesized activated carbons, we can usually mention two types of pores. Table 2 shows that activated carbons are composed of micropore and mesopore. Some samples were found to consist entirely of micropores. In particular, the activated carbon synthesized at low carbonization temperature and low activation temperature is entirely composed of micropores. Increased carbonization temperature increased mesopore formation. Also, the increased gas flow rate increased the amount of mesopore in the samples. Another parameter, namely activation temperature, positively affected mesopore formation. Table 2 shows the total volume, micro and meso volumes of the activated carbons. Almost all of the samples consisted of micro volumes. In some samples, meso volumes were not observed at all, whereas in some samples a small amount was observed. Increased activation temperature caused micro volume to increase.

In the literature (42), activated carbon synthesis have been made from peach kernel shell. However, chemical activation method was generally used in these studies. In very few physical activation the results of activation temperature and carbonization temperature on activated carbon using CO_2 were not investigated. In some studies, physical activation was performed with water vapor. However, even with this activation, the activated carbons synthesized differ from each other. Compared with the studies in the literature, this study showed differences in many ways. The surface areas of the synthesized activated carbons were smaller than those synthesized by chemical activation in the literature (43). This is due to the fact that the chemical agent can directly contact the surface while the CO_2 hits the surface. However, during this contact, the chemical agent affected the surface and the active carbons have increased the ratio of mesopore. In this study, the amount of mesopore is less. In the literature (31), water vapor is used in activated carbons synthesized by physical activation. It is seen that the use of water vapor

causes more development of pores. When the water molecule contacted the biomass, it caused the pores to grow by contacting the pore walls in the cavities formed by carbonization. However, since the CO_2 molecule was larger than the water molecule, it could not provide expansion in the walls and expanded into the pore center. Therefore, the amount of mesopore is very high in water vapor studies in the literature. As the surface area will increase with increasing mesopore amount, the surface area in these studies is higher than the surface areas of the synthesized active carbons.

Figure 1 shows that the pore distribution ranges in the samples. Samples generally have pore distributions ranging from 1 nm to 2 nm. These pore distributions show the micropores formed in the structure. As in Table 2, the micropore ratio was found to be high in the samples. These results showed parallelism with the pore distribution graph and confirmed the structure.

One of the ways of characterizing activated carbons is N2 adsorption graphs. N2 adsorption graphs provide information about the pores of activated carbons. Six types of adsorption plots were defined by IUPAC (International Union of Pure and Applied Chemistry). Each graph tells us about the pores of activated carbons by following different N2 adsorption. N2 adsorption graphs of the synthesized activated carbons are given in Figure 2. According to the graph in Figure 2, the N2 adsorption graph is similar to type 1. Type 1 graphs are generally N2 adsorption graphs seen in microporous and low surface area activated carbons. In the graph, adsorption at low pressure increases rapidly. This increase is due to microporous. The adsorption stops with the filling of micropores in the structure and the graph proceeds in a straight way.

Table 2: BET analysis results of activated carbons.

| Carbonization | | Physical Activation | | | | | | | |
Temp. (°C)	N₂ Gas Flow (min/mL)	Temp. (°C/100 mL CO₂)	S_{BET} m²/g	S_{micro} m²/g	S_{meso} m²/g	V_T cm³/g	V_{micro} cm³/g	V_{meso} cm³/g	dp nm
300	100	800	340.15	340.15	-	0.19	0.17	0.02	-
300	500	800	353.48	353.48	-	-	0.18	-	-
300	100	900	445.42	412.06	33.35	0.22	0.21	0.01	2
300	500	900	417.42	408.03	9.38	0.20	0.21	-	1.94
400	100	800	596.73	69.81	526.9	0.55	0.03	0.52	3.74
400	500	800	378.05	373.27	4.78	0.18	0.19	-	1.92
400	100	900	458.24	426.67	31.56	0.228	0.224	0.004	1.99
400	500	900	451.8	427.63	24.17	-	0.22	-	-
500	100	800	686.74	-	686.7	0.68	0.02	0.66	4.01
500	500	800	356.99	356.99	-	-	0.19	-	-
500	100	900	422.53	402.39	20.13	0.20	0.21	-	1.97
500	500	900	447.65	412.41	35.23	0.22	0.21	0.01	1.99
600	100	800	349.23	343.24	5.98	0.18	0.05	0.13	-
600	500	800	345.42	345.42	-	-	0.18	-	-
600	100	900	427.13	399.99	27.14	0.21	0.21	-	2
600	500	900	412.89	409	3.88	-	0.21	-	-
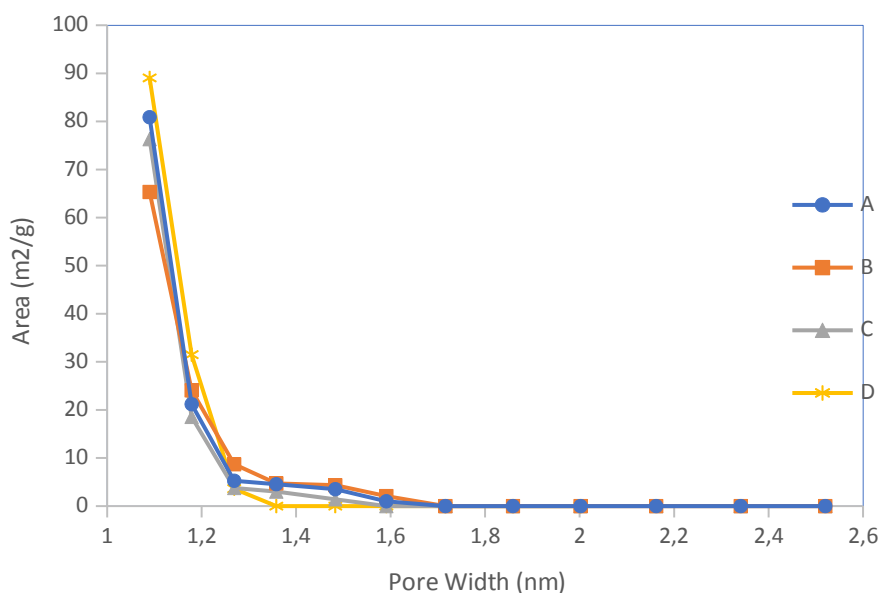
Figure 1: Pore size distribution of activated carbon sample A. Activated carbon sample at 500 °C 100 mL/min N_2 carbonization and at 900 °C with 100 mL/min CO_2 activation B. Activated carbon sample at 400 °C 100 mL/min N_2 carbonization and at 900 °C with 100 mL/min CO_2 activation C. Activated carbon sample at 600 °C 100 mL/min N_2 carbonization and at 800 °C with 100 mL/min CO_2 activation   D. Activated carbon sample at 300 °C 100 mL/min N_2 carbonization and at 800 °C with 100 mL/min CO_2 activation.
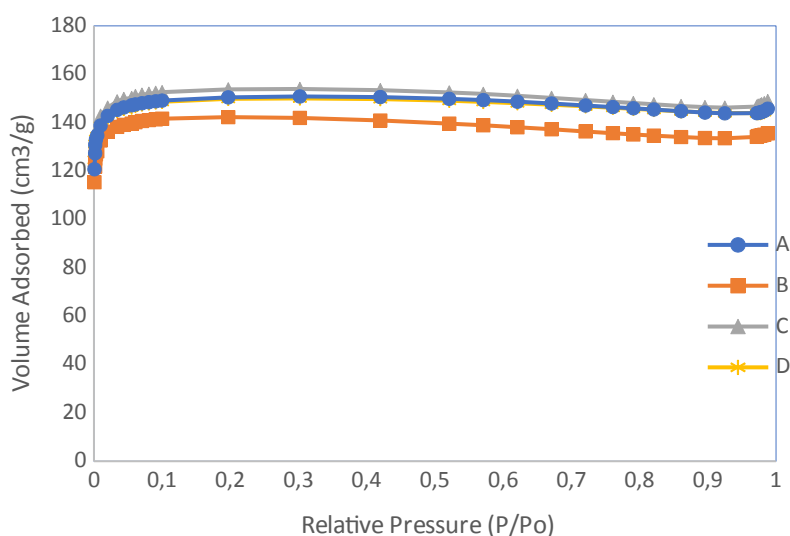
Figure 2: Adsorption isotherms of N_2 A. Activated carbon sample at 500 °C 500 mL/min N_2 carbonization and at 900 °C with 100 mL/min CO_2 activation B. Activated carbon sample at 500 °C 100 mL/min N_2 carbonization and at 900 °C with 100 mL/min CO_2 activation C. Activated carbon sample at 400 °C 100 mL/min N_2 carbonization and at 900 °C with 100 mL/min CO_2 activation D. Activated carbon sample at 300 °C 100 mL/min N_2 carbonization and at 900 °C with 100 mL/min CO_2 activation.
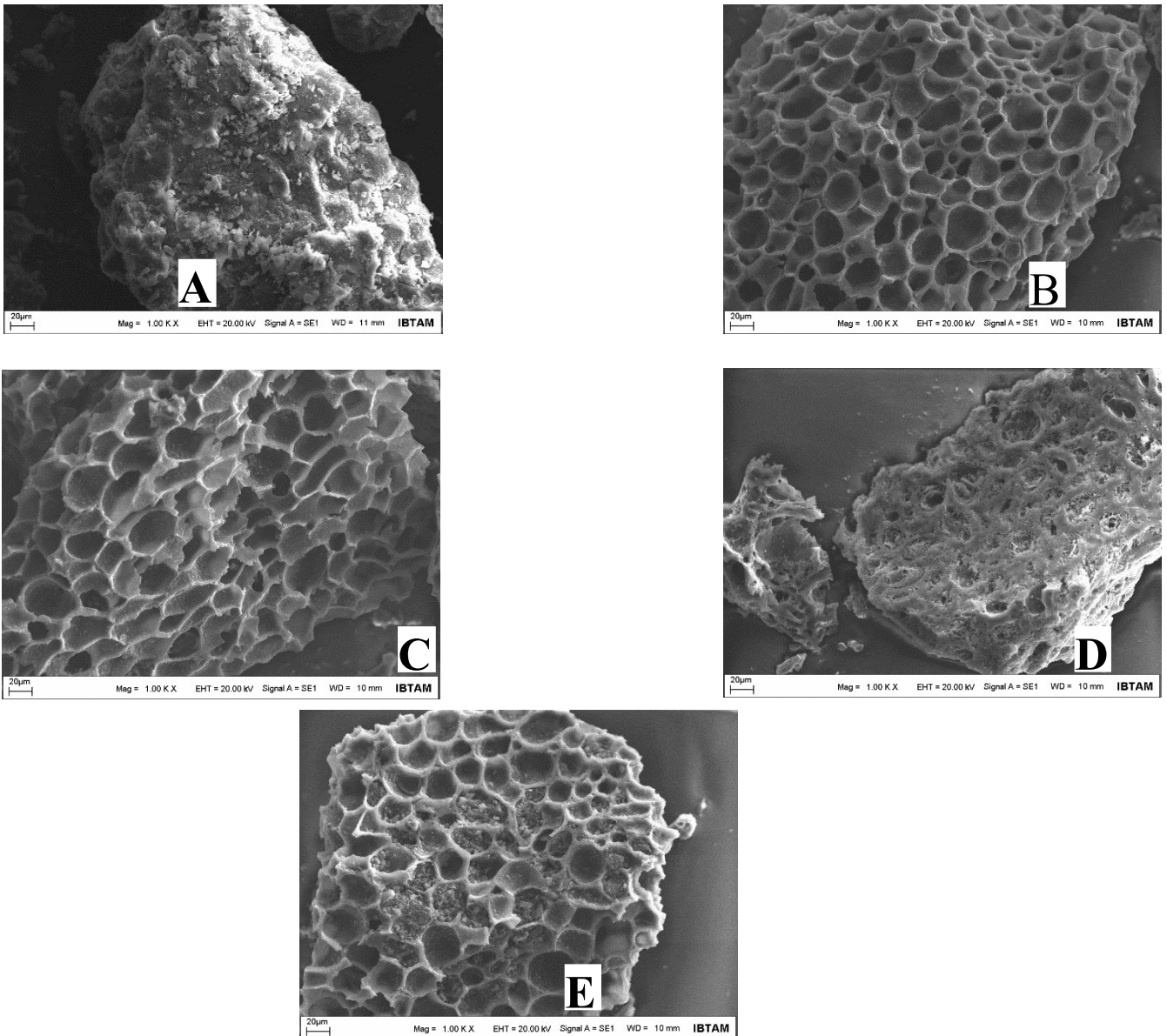
Figure 3: A. SEM image of raw peach shell B. Activated carbon sample at 500 °C 100 mL/min N_2 carbonization and at 800 °C with 100 mL/min CO_2 activation C. Activated carbon sample at 500 °C 500 mL/min N_2 carbonization and at 900 °C with 100 mL/min CO_2 activation. D. Activated carbon sample at 400 °C 100 mL/min N_2 carbonization and at 800 °C with 100 mL/min CO_2 activation. E. Activated carbon sample at 400 °C 100 mL/min N_2 carbonization and at 900 °C with 100 mL/min CO_2 activation.
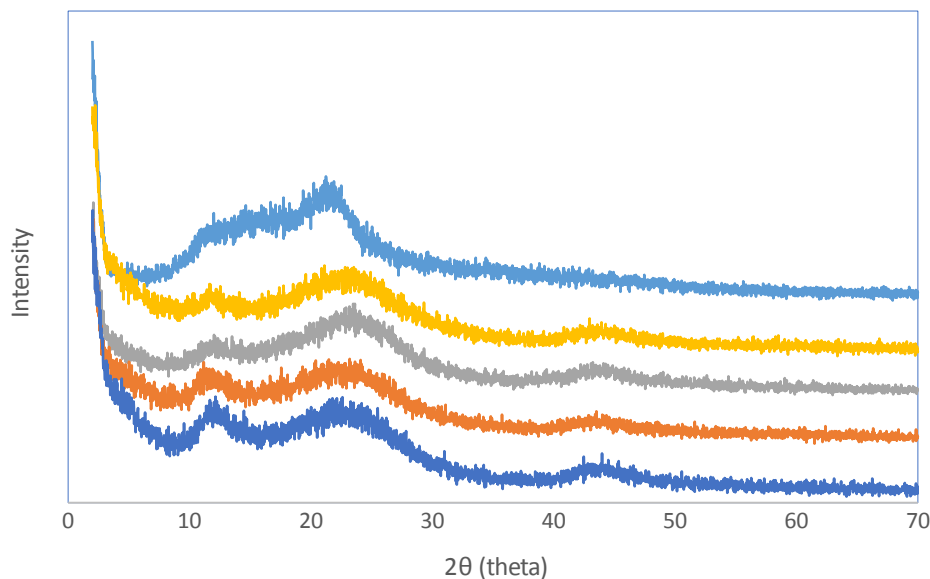
Figure 4: XRD chart of samples. A. XRD chart of raw peach shell. B. Activated carbon sample at 400 °C 100 mL/min N_2 carbonization and at 800 °C with 100 mL/min CO_2 activation. C. Activated carbon sample at 400 °C 100 mL/min N_2 carbonization and at 900 °C with 100 mL/min CO_2 activation. D. Activated carbon sample at 500 °C 100 mL/min N_2 carbonization and at 800 °C with 100 mL/min CO_2 activation. E. Activated carbon sample at 500 °C 500 mL/min N_2 carbonization and at 900 °C with 100 mL/min CO_2 activation
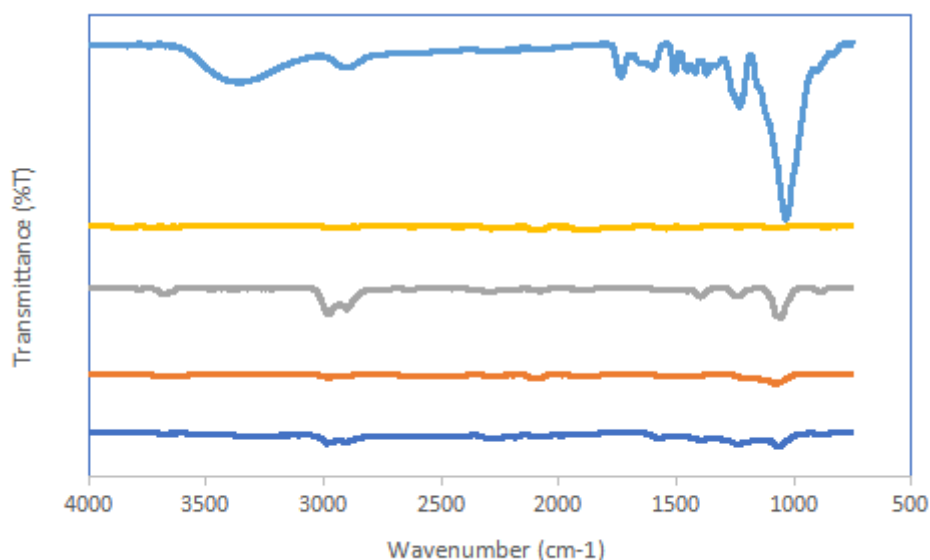
Figure 5: FTIR spectra of raw material and activated carbon samples. A. Raw material. B. Activated carbon sample at 400 °C 100 mL/min N_2 carbonization and at 800 °C with 100 mL/min CO_2 activation. C. Activated carbon sample at 400 °C 100 mL/min N_2 carbonization and at 900 °C with 100 mL/min CO_2 activation. D. Activated carbon sample at 500 °C 100 mL/min N_2 carbonization and at 800 °C with 100 mL/min CO_2 activation. E. Activated carbon sample at 500 °C 500 mL/min N_2 carbonization and at 900 °C with 100 mL/min CO_2 activation.

One of the methods used to characterize activated carbons is SEM analysis. Thanks to SEM analysis, we see the pores of the activated carbons. SEM images of the synthesized activated carbons and peach kernel shell used as raw materials are shown in Figure 3. According to SEM images, peach kernel shell does not show pores on its surface without any pretreatment. The formation of pores on the surface is seen as a result of activated carbon synthesis.

XRD analysis of synthesized activated carbons and peach kernel shell is shown in Figure 4. When the raw materials and activated carbons were examined, no crystalline structure was found in the

structure. Amorphous is observed in the structures. In the peach kernel shell used in the synthesis of activated carbon, a small amount of regular structure is encountered. In particular, the peak of about 22° is defined as the cellulose peak and is seen in cellulose-structured materials. During the synthesis of activated carbon, this regular structure was disrupted by heat and partially lost this peak intensity in activated carbon samples.

The FTIR spectroscopy technique was used to identify the functional groups on the surface on activated carbons and the raw material. According to the FTIR spectra in Figure 5, the band belongs to OH stress vibrations at approximately 3450 cm^{-1}, band around 2850 cm^{-1} indicates the C-H stretching vibrations, the band seen at about 1700 cm^{-1} originates from C=O, band at about 1600 cm^{-1} belongs to the C=C bond vibration of alkenes. Band at about 1000 cm^{-1} is the peak of vibrations caused by C-OH and C-O-C bonds.

Elemental analysis results of synthesized activated carbons and raw material are given in Table 3. According to Table 3, It is seen that the carbon amounts of the synthesized activated carbons are approximately 7-71% higher than the raw materials. In addition, the carbon content of the synthesized activated carbons that are exposed to a high activation temperature is generally less than the others. Activated carbons synthesized at the same carbonization temperature and activation temperature of 800 °C appear to reduce the amount of carbon at an increased gas flow rate. However, at the activation temperature of 900 °C this was the opposite. The hydrogen content of the synthesized active carbons decreased approximately 5 times compared to the raw material.

Adsorption, which is one of the most commonly used application fields of activated carbons, was studied. In this work, methylene blue adsorption capacities of activated carbons were examined. The adsorption capacity of the synthesized activated carbons was found to be very low. The reason for this is methylene blue, which is the molecule to be adsorbed, and the reason is the diameter of the pores formed on the activated carbon. If the molecule to be adsorbed passes through the pores on the activated carbon, it will bind to the atoms on the outer surface of the pores through secondary interactions. Because the methylene blue molecule did not pass through the pores on the activated carbon this phenomenon could not occur. The synthesized activated carbons have very small pore diameters. DFT results show how small and narrow the pore diameters change. Therefore, these results are quite natural.

CONCLUSIONS

In this study, it is aimed to synthesize activated carbon with narrow pore distribution from peach seed peel, which is an agricultural waste. In the study, carbonization was made at 4 different temperatures and 2 different gas flows, and CO2 was used for activation. As a result of the characterization of the samples, it was observed that micropores were abundant and showed a narrow pore distribution according to the DFT plus data. The micropore ratio in the prepared activated carbons varied depending on the temperature and gas flow rate. No micropores were observed in one sample, although some samples consisted entirely of micropores. In the elemental analysis of activated carbons, the amount of carbon showed a maximum increase of 71% compared to the raw material. In the study, the adsorption capacity of methylene blue studied in the samples with narrow pore distribution was quite low, while adsorption was not observed in some samples. Although the activated carbons prepared in this study are not suitable for methylene blue adsorption, it can be checked whether they are suitable by using different applications.

Table 3: Elementary analysis results of raw materials and activated carbons.

Carbonization		Physical Activation				
Temperature °C	N$_2$ Gas Flow dk/mL	Temperature (°C/100 mL CO$_2$)	C	H	N	S
Raw Materials			50.45	5.68	0.072	-
300	100	800	79.27	1.03	0.28	-
300	500	800	78.25	1.132	0.32	-
300	100	900	54.07	1.317	0.184	-
300	500	900	57.74	1.063	0.242	-
400	100	800	86.27	0.98	-	-
400	500	800	74.85	1.628	0.276	-
400	100	900	62.06	0.59	-	-
400	500	900	69.40	1.219	0.132	-
500	100	800	86.53	0.97	-	-
500	500	800	79.76	1.607	0.268	-
500	100	900	65.90	1.509	0.138	0.053
500	500	900	74.34	0.64	-	-
600	100	800	84.00	1.39	0.215	-
600	500	800	77.46	1.412	0.259	-
600	100	900	76.81	0.59	-	-
600	500	900	82.77	1.009	0.173	0.054

Table 4: Methylene blue adsorption capacity of activated carbons.

Carbonization		Physical Activation		
Temperature °C	N$_2$ Gas Flow dk/mL	Temperature (°C/100 mL CO$_2$)	S$_{BET}$ m^2/g	Adsorption Capacity q$_e$ (mg/g)
300	100	800	340.15	2.98
300	500	800	353.48	0.89
300	100	900	445.42	12
300	500	900	417.42	9.69
400	100	800	596.73	1.44
400	500	800	378.05	-
400	100	900	458.24	24.1
400	500	900	451.8	16.29
500	100	800	686.74	-
500	500	800	356.99	-
500	100	900	422.53	9.69
500	500	900	447.65	7.74
600	100	800	349.23	-
600	500	800	345.42	-
600	100	900	427.13	8.15
600	500	900	412.89	7.93

REFERENCES

1. Ayinla RT, Dennis J, Zaid H, Sanusi Y, Usman F, Adebayo L. A review of technical advances of recent palm bio-waste conversion to activated carbon for energy storage. Journal of cleaner production. 2019;229:1427-42. <DOI>

2. Mayyas M, Sahajwalla V. Carbon nano-sponge with enhanced electrochemical properties: A new understanding of carbon activation. Chemical Engineering Journal. 2019;358:980-91. <DOI>

3. Khan JH, Marpaung F, Young C, Lin J, İslam MT, Alsheri SM, Ahamad T, Alhokbany N, Ariga K, Shrestha LK, Yamauchi Y, W. Wu KC, Hossain MSA, Kim J. Jute-derived microporous/mesoporous carbon with ultra-high surface area using a chemical activation process. Microporous Mesoporous Materials. 2019;274:251-6. <DOI>

4. Zhang Y, Song X, Xu Y, Shen H, Kong X, Xu H. Utilization of wheat bran for producing activated carbon with high specific surface area via NaOH activation using industrial furnace. Journal of cleaner production. 2019;210:366-75. <DOI>

5. Sharma M, Joshi M, Nigam S, Shree S, Avasthi DK, Adelung R, Srivastava SK, Mishra YK. ZnO tetrapods and activated carbon based hybrid composite: Adsorbents for enhanced decontamination of hexavalent chromium from aqueous solution. Chemical Engineering Journal. 2019;358:540-51. <DOI>

6. Abdullah MO, Tan IW, Lim LS. Automobile adsorption air-conditioning system using oil palm biomass-based activated carbon: a review. Renewable Sustainable Energy Reviews. 2011; 15:2061-72. <DOI>

7. Hu Z, Srinivasan M. Mesoporous high-surface-area activated carbon. Microporous Mesoporous Materials. 2001;43:267-75. <DOI>

8. Sinha P, Banerjee S, Kar K.K. Characteristics of activated carbon. Springer Series in Materials Science. 2020. ISBN: 978-3-030-43009-2

9. Oliveira L, Pereira E, Guimaraes R, Vallone A, Pereira M, Mesquita JP, Sapag K. Preparation of activated carbons from coffee husks utilizing FeCl3 and ZnCl2 as activating agents. Journal of Hazardous Materials. 2009;165;87-94. <DOI>

10. Chandra TC, Mirna M, Sudaryanto Y, Ismadji S. Adsorption of basic dye onto activated carbon prepared from durian shell: Studies of adsorption equilibrium and kinetics. Chemical Engineering Journal. 2007;127:121-9. <DOI>

11. Martinez ML, Torres MM, Guzman CA, Maestri DM. Preparation and characteristics of activated carbon from olive stones and walnut shells. Industrial crops products. 2006;23:23-8. <DOI>

12. Gao P, Liu Z-H, Xue G, Han B, Zhou M-H. Preparation and characterization of activated carbon produced from rice straw by (NH4) 2HPO4 activation. Bioresource technology.2011;102:3645-8. <DOI>

13. Foo K, Hameed B, Microwave-assisted preparation of oil palm fiber activated carbon for methylene blue adsorption. Chemical Engineering Journal. 2011;166:792-5. <DOI>

14. Gonzalez JF, Roman S, González-García CM, Nabais JV, Ortiz AL. Porosity development in activated carbons prepared from walnut shells by carbon dioxide or steam activation. Industrial engineering chemistry research. 2009;48:7474-81. <DOI>

15. Chen Y, Zhu Y, Wang Z, Li Y, Wang L, Ding L, Gao X, Ma Y, Guo Y. Application studies of activated

carbon derived from rice husks produced by chemical-thermal process—A review, Advances in colloid interface science, 2011;163:39-52. <DOI>

16. Demirbas E, Kobya M, Sulak M. Adsorption kinetics of a basic dye from aqueous solutions onto apricot stone activated carbon. Bioresource technology. 2008;99:5368-73. <DOI>

17. Angin D. Production and characterization of activated carbon from sour cherry stones by zinc chloride. Fuel. 2014;115:804-11. <DOI>

18. Van Thuan T, Quynh BTP, Nguyen TD, Bach LG. Response surface methodology approach for optimization of Cu^{2+}, Ni^{2+} and Pb^{2+} adsorption using KOH-activated carbon from banana peel. Surfaces Interfaces. 2017;6:209-17. <DOI>

19. Srinivasakannan C, Bakar MZA. Production of activated carbon from rubber wood sawdust. Biomass and Bioenergy.2004;27;89-96. <DOI>

20. Suzuki R, Andrade A, Sousa J, Rollemberg M. Preparation and characterization of activated carbon from rice bran. Bioresource technology. 2007;98:1985-91. <DOI>

21. Mohan D, Sarswat A, Singh VK, Alexandre-Franco M, Pittman Jr. C. Development of magnetic activated carbon from almond shells for trinitrophenol removal from water. Chemical Engineering Journal. 2011;172:1111-25. <DOI>

22. Yagmur E, Ozmak M, Aktas Z. A novel method for production of activated carbon from waste tea by chemical activation with microwave energy. Fuel. 2008;87:3278-85. <DOI>

23. Yang J, Qiu K. Development of high surface area mesoporous activated carbons from herb residues. Chemical engineering journal. 2011;167:148-54. <DOI>

24. Bagheri N, Abedi J, Adsorption of methane on corn cobs based activated carbon. Chemical Engineering Research Design. 2011;89:2038-43. <DOI>

25. Teker M, Saltabaş Ö, İmamoğlu M. Adsorption of cobalt by activated carbon from the rice hulls. Journal of Environmental Science Health Part A. 1997;32:2077-86. <DOI>

26. Krishnan KA, Anirudhan T. Uptake of heavy metals in batch systems by sulfurized steam activated carbon prepared from sugarcane bagasse pith. Industrial Engineering Chemistry Research. 2002;41:5085-93. <DOI>

27. Deng H, Zhang G, Xu X, Tao G, Dai J. Optimization of preparation of activated carbon from cotton stalk by microwave assisted phosphoric acid-chemical activation. Journal of Hazardous Materials. 2010;182:217-24. <DOI>

28. Fernandez ME, Nunell GV, Bonelli PR, Cukierman AL. Activated carbon developed from orange peels: Batch and dynamic competitive adsorption of basic dyes. Industrial Crops Products. 2014;62:437-45. <DOI>

29. Alhamed YA. Adsorption kinetics and performance of packed bed adsorber for phenol removal using activated carbon from dates' stones. Journal of Hazardous Materials. 2009;170:763-70. <DOI>

30. Gupta VK, Jain R, Shrivastava M, Nayak A. Equilibrium and thermodynamic studies on the adsorption of the dye tartrazine onto waste "coconut husks" carbon and activated carbon. Journal of Chemical Engineering Data. 2010;55:5083-90. <DOI>

31. Pallares J, Cencerrado GA, Arauzo I. Production and characterization of activated carbon from barley straw by physical activation with carbon dioxide and steam. Biomass and Bioenergy. 2018;115:64-73. <DOI>

32. Jurado-Sanchez B, Sattayasamitsathit S, Gao W, Santos L, Fedorak Y, Sing Vv, Orozco J, Galarnyk M, Wang J. Self-Propelled Activated Carbon Janus Micromotors for Efficient Water Purification. Small. 2015;11:499-506. <DOI>

33. Matsuo T, Nishi T. Activated carbon filter treatment of laundry waste water in nuclear power plants and filter recovery by heating in vacuum. Carbon. 2000;38(5):709-14. <DOI>

34. Sircar S, Golden T, Rao M. Activated carbon for gas separation and storage. Carbon. 1996;34(1):1-12. <DOI>

35. Fang B, Binder L. A modified activated carbon aerogel for high-energy storage in electric double layer capacitors. Journal of power sources. 2006;163; 616-22. <DOI>

36. Faria P, Órfão J, Pereira M. Activated carbon catalytic ozonation of oxamic and oxalic acids. Applied Catalysis B: Environmental. 2008;79:237-43. <DOI>

37. Rivera-Utrilla J, Sánchez-Polo M, Gómez-Serrano V, Alvarez P, Alvim-Ferraz M, Dias J. Activated carbon modifications to enhance its water treatment applications. An overview. Journal of hazardous materials. 2011;187:1-23. <DOI>

38. Snyder AS, Adham S, Redding AM, Cannon FS, Decarolis J, Oppenheimer J, Wert EC, Yoon Y. Role of membranes and activated carbon in the removal of endocrine disruptors and pharmaceuticals, Desalination, 2007;202:156-81. <DOI>

39. Park JH, Park OO. Hybrid electrochemical capacitors based on polyaniline and activated carbon electrodes. Journal of Power Sources. 2002;111:185-0. <DOI>

40. Anirudhan T, Sreekumari S, Bringle C. Removal of phenols from water and petroleum industry refinery effluents by activated carbon obtained from coconut coir pith. Adsorption. 2009;15;439. <DOI>

41. Vargas AM, Cazetta AL, Kunita MH, Silva TL, Almeida VC. Adsorption of methylene blue on activated carbon produced from flamboyant pods (Delonix regia): Study of adsorption isotherms and kinetic models. Chemical Engineering Journal. 2011;168:722-30. <DOI>

42. Anyika C, Asri NAM, Majid ZA, Yahya A, Jaafar J. Synthesis and characterization of magnetic activated carbon developed from palm kernel shells. Nanotechnology for Environmental Engineering. 2017; 2: 16. <DOI>

43. Prauchner JM, Sapag K, Reinoso RF. Tailoring biomass-based activated carbon for CH4 storage by combining chemical activation with H3PO4 or ZnCl2 and physical activation with CO2. 2016;110:138-47. <DOI>